Which is smoother: the sphere or the cone?

P. F. Embid[1,2], **J. H. Cooley**[2], **and D. M. Topa**[1,2]
[1]Department of Mathematics and Statistics, University of New Mexico, Albuquerque, NM, USA
[2]Los Alamos National Laboratory, Los Alamos, NM, USA

Abstract— *We studied the smoothness of a hemisphere and cone using a Zernike polynomial expansion. This is akin to characterizing the regularity of a function in Fourier analysis. The polynomial expansion amplitudes were computed analytically and compared for the two surfaces. Also, the maximum residual errors were compared. The results were unexpected.*

Keywords: Zernike polynomials, regularity, Weierstrass approximation theorem

1. Introduction

This paper looks at representations of the cone $A(r)$ and the sphere $B(r)$ in the Zernike radial polynomial basis. This basis spans a complete, separable Hilbert space over $\overline{D}_2$, the closed unit disk. More precisely, we look at the right circular cone and the hemisphere described here

$$\begin{aligned} A(r) &= 1 - r, \\ B(r) &= \sqrt{1 - r^2}, \end{aligned} \tag{1}$$

over the domain $0 \leq r \leq 1$. We compute the amplitudes, and the maximum error over the domain, as a function of expansion order n.

The study was motivated by a desire to compare the amplitudes for a smooth object, the sphere, with the amplitudes for a smooth object with a single, well-defined blemish, the cone. The hope was that this would be a useful pedagogical exercise in approximation theory. We have succeeded in creating such an example, but for an entirely different set of reasons. The results were counterintuitive and they have provided delightful insight.

The sphere is the archetypical surface of constant phase as it represents the wavefront from a point source. Much of optics theory, measurement and metrology revolves around determining the curvature of spherical wavefronts. So the sphere is an ideal starting point for Zernike decomposition.

We wanted a second smooth function, but with a single blemish. The anticipation was that the abrupt change in the Zernike amplitudes would provide insight into the significance of the decomposition. The cone is a smooth function except for the sharp discontinuity at the apex. The cone is also a surface of constant phase as it represents the Ĉerenkov wavefront from an inertial point source.

2. Theory

This section introduces the polynomials orthogonal over the unit disk and provides the background which justifies and quantifies the behavior of the polynomial expansion.

2.1 The disk polynomials of Zernike

The disk polynomials of Zernike [1] are a complete basis set orthogonal on the closed unit disk $\overline{D}_2 = \{z \in \mathbb{C} \colon |z| \leq 1\}$. We use the complex representation given in Born and Wolf [2, Appendix VII, eqn. 7] and Bhatia and Wolf [3, eqn. 2.18]:

$$V_n^m(r,\theta) = R_n^m(r) e^{im\theta}. \tag{2}$$

Here n represents the order and m represents an angular frequency. Note that $n - m$ is always even. The Zernike decomposition for an arbitrary continuous function $\psi(r,\theta)$ over the unit disk evokes similarity to a Fourier decomposition

$$\psi(r,\theta) = \sum_{n=0}^{\infty} \sum_{m=-n}^{n} a_n^m R_n^m(r) e^{im\theta}. \tag{3}$$

When we define the variable

$$\Delta_{\pm} = \frac{1}{2}(n \pm m) \tag{4}$$

then the radial functions have this form:

$$R_n^m(r) = \sum_{k=0}^{\Delta_-} (-1)^k \frac{(n-k)!}{k!\,(\Delta_+ - k)!\,(\Delta_- - k)!} r^{n-2k}. \tag{5}$$

In this analysis, we are interested in the rotationally invariant terms, those with angular velocity $m = 0$. This reduced set is dense in the space of rotationally invariant functions on the unit disk and is given by the following relationship:

$$R_n^0(r) = \sum_{k=0}^{n/2} (-1)^k \frac{(n-k)!}{k![(n/2-k)!]^2} r^{n-2k}. \tag{6}$$

A sample basis through order $n = 6$ takes the form

$$\begin{aligned} \{z_0(r), z_2(r), z_4(r), z_6(r)\} &= \\ &= \left\{1, 2r^2 - 1, 6r^4 - 6r^2 + 1, \right. \\ &\qquad \left. 20r^6 - 30r^4 + 12r^2 - 1\right\}. \end{aligned} \tag{7}$$

Notice that this is just a Gram-Schmidt orthogonalization of radial polynomials of even order $\{1, r^2, r^4, \dots\}$ over the domain $0 \leq r \leq 1$ with unit weighting and normalization $z_n(1) = \pm 1$.

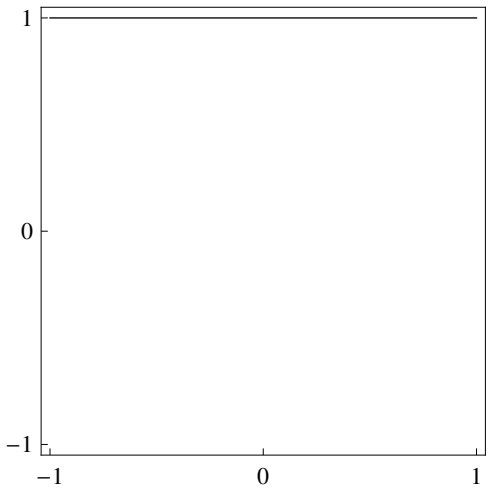

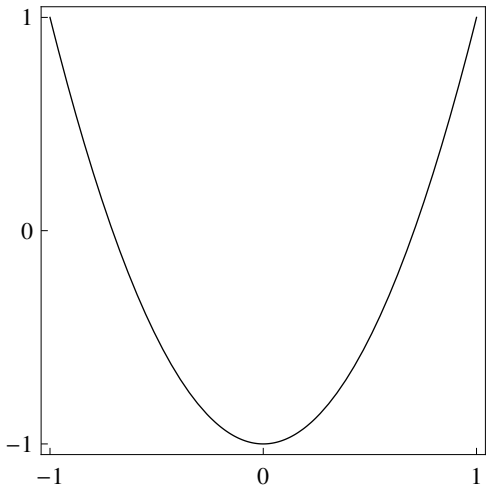

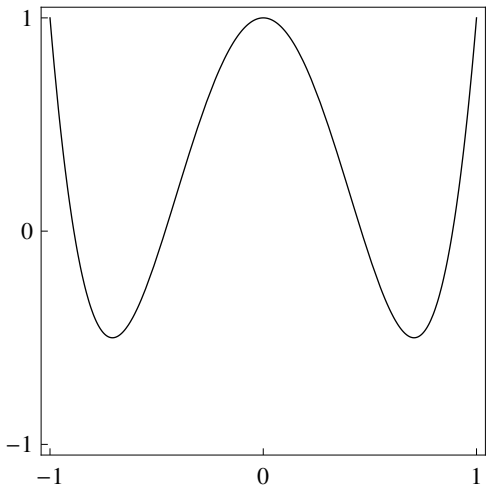

Fig. 1: A look at the radial polynomials of lowest order $n = 0, 2, 4$.

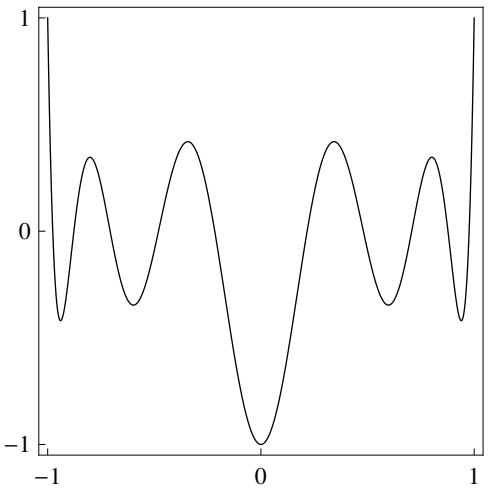

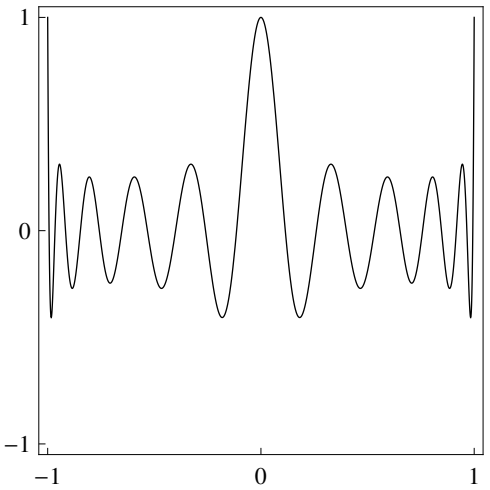

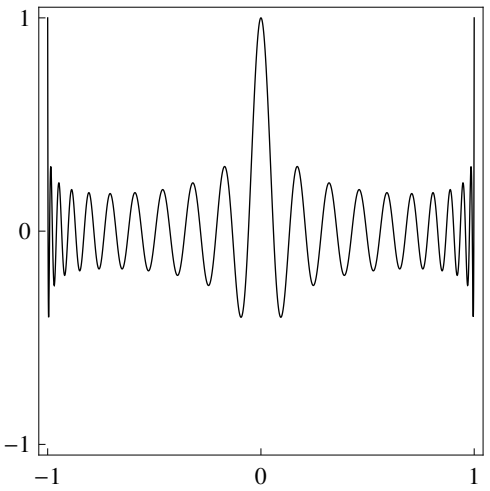

Fig. 2: A look at some higher power radial polynomials $n = 10, 20, 40$.

A few of the radial polynomials are plotted in figures (1) and (2). Notice the similarity to a Fourier cosine sequence. The first term represents a constant offset and subsequent terms introduce higher frequency oscillations.

In this paper we consider two basic measurements, each with a different norm. The amplitudes were computed using the L^2 norm; the uniform error represents the L^∞ norm.

2.2 The approximation theory of Weierstrass

The foundation for polynomial approximation is the Weierstrass Approximation Theorem [4] which in essence states:

> The polynomials are dense in the space of continuous functions with respect to the uniform norm.

The implication is that any piecewise continuous (C^0) function can be *uniformly* approximated by a sequence of polynomials over a finite interval. A sequence of polynomial functions $\{f_k(r)\}_{k=0}^{\infty}$ converges uniformly on $\overline{D}_2$ to a function $f(r)$ if for every $\epsilon > 0$ there is an integer N such that $n \geq N$ implies

$$|f(r) - f_n(r)| \leq \epsilon \tag{8}$$

for all values of r in the domain. The crucial concept is that the error ϵ is a constant for the entire domain and does not depend upon the variable r. In section (3.3) we present an explicit calculation for the parameter N.

2.3 Method

The two methods below rely upon two different norms. The amplitudes are found using the method of least squares and hence use the L^2 norm. The maximum errors between the input surface and the approximation represents the L^∞ norm.

2.3.1 Computing the amplitudes

We use projection to compute the Zernike amplitudes for each surface. These amplitudes are the least squares solutions found using the orthogonality relationship

$$\int_0^{2\pi}\int_0^1 R_n^0(r)R_m^0(r)\,r dr d\theta = \frac{\pi}{n+1}\delta_n^m \tag{9}$$

where both n and m are even integers.

For example, consider the nth order approximation polynomial for the cone

$$\begin{aligned} a_n(r) &= \alpha_0 R_0^0(r) + \alpha_2 R_2^2(r) + \cdots + \alpha_n R_0^n(r) \\ &= \sum_{k=0}^{n/2} \alpha_{2k} R_{2k}^0(r). \end{aligned} \tag{10}$$

The individual amplitudes are

$$\alpha_n = \frac{\int_0^1 A(r) R_n^0\, r dr}{\int_0^1 R_n^0 R_n^0\, r dr}. \tag{11}$$

These amplitudes α are the set which minimize the L^2 norm of the error over the domain:

$$\min_{\alpha\in\mathbb{R}^{n/2+1}} \int_0^{2\pi}\int_0^1 |A(r) - a_n(r)|^2\, r dr d\theta. \tag{12}$$

The Zernike basis is well-suited for representation, yet ill-suited for computation. If we forego the Zernike basis and use the even polynomials in the radial variable r, we can compute the integrals analytically using these scalars:

$$\begin{aligned} \xi_n &= \int_0^1 (1-r)\, r^n r dr = \frac{1}{(n+2)\,(n+3)}, \\ \eta_n &= \int_0^1 \sqrt{1-r^2} r^n r dr = \frac{\sqrt{\pi}}{4}\frac{\Gamma\left(\frac{n+2}{n}\right)}{\Gamma\left(\frac{n+5}{n}\right)}. \end{aligned} \tag{13}$$

We can avoid integrands built with computationally expensive Zernike polynomials and instead employ the even radial polynomials. For the Zernike *polynomials* substitute the corresponding coordinate *vector* in the monomial basis. As an example compute the numerator in equation (11) for α_4:

$$\begin{aligned} &\int_0^1 (1-r)\, R_4^0(r) r dr = \int_0^1 (1-r)\left(1 - 6r^2 + 6r^4\right) r dr \\ &= \int_0^1 (1-r)\, r dr - 6\int_0^1 r^2\,(1-r)\, r dr + 6\int_0^1 r^4\,(1-r)\, r dr \\ &= (z(4))\cdot(\xi_0,\xi_2,\xi_4) = (1,-6,6)\cdot\left(\frac{1}{6},\frac{1}{20},\frac{1}{42}\right) = \frac{1}{105}. \end{aligned} \tag{14}$$

2.3.2 Computing the maximum error

The residual fit error of the cone for the nth order is expansion is given by

$$\epsilon_n(r) = A(r) - a_n(r). \tag{15}$$

The L^∞ error is the maximum of this residual error over the domain:

$$\max_{0\leq r\leq 1} |A(r) - a_n(r)|\,. \tag{16}$$

3. Results

The results were counterintuitive. The magnitude of the amplitudes is exactly the same for both surfaces. The magnitude of the maximum residual error is also exactly the same. A few terms of the reconstruction sequence are shown in figures (3) and (4).

3.1 Smoothness of the functions

The amplitudes were computed for both surfaces through order 50,000. Also, the L^∞ error was computed for each surface through the same order. The amplitudes for the cone are α_n and the amplitudes for the hemisphere are β_n. Table (1) below shows the Zernike amplitudes for order $n = 0, 2, \ldots, 20$. The first term represents the average value for the surface and do not affect its shape. We could add

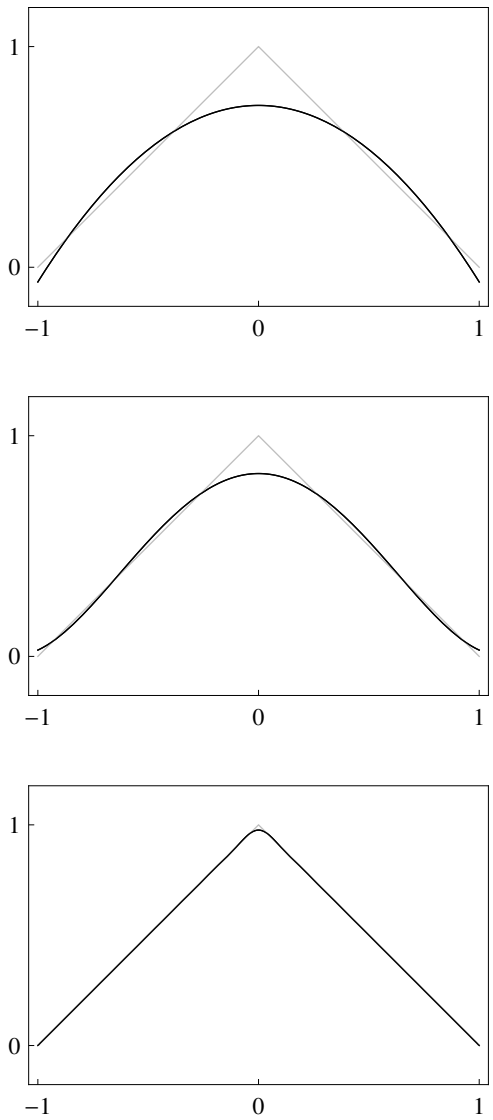

Fig. 3: Approximating the cone. These are the approximations for order $n = 2, 4, 40$.

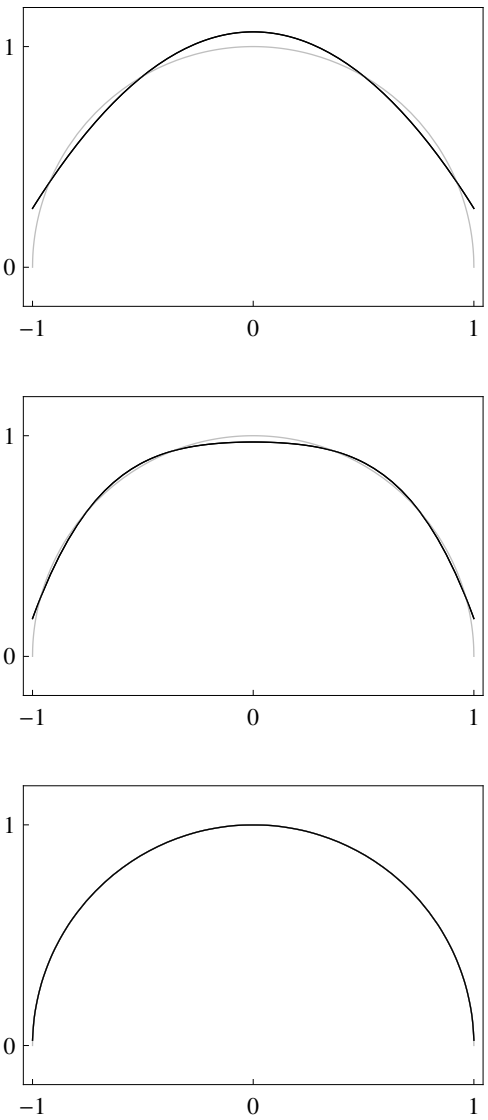

Fig. 4: Approximating the sphere. These are the approximations for order $n = 2, 4, 40$.

a constant offset to either surface and force an equality of these terms; however, this would have introduced a needless term into one of the functional forms.

We find a quadratic decay of the amplitudes. (A surface with cubic decay would be smoother.) For $n = 2, 4, 6, \ldots$

$$\beta_n = -\frac{2}{(n+3)\,(n-1)} \tag{17}$$

The surprising discovery is that the amplitudes for the sphere and the cone have exactly the same magnitude. Specifically, for $n = 2, 4, 6, \ldots,$

$$\alpha_n = (-1)^{k+1}\,\beta_n. \tag{18}$$

This implies the equality of these integrals:

$$\int_0^1 \sqrt{1-r^2} R_n^0\, r dr = (-1)^{k+1} \int_0^1 (1-r)\, R_n^0\, r dr \tag{19}$$

for $n = 0, 2, 4, \ldots$.

3.2 Accuracy of the reconstruction

We want to quantify the accuracy of each approximation using the uniform or L^∞ norm of equation (16). This measures the largest difference between the function and the approximation over the entire domain. Here too the

Table 1: The first few amplitudes from the expansion as a function of the order n. The α values correspond to the cone, β to the sphere.

n	α	β
0	$\frac{1}{3}$	$\frac{2}{3}$
2	$-\frac{2}{5}$	$-\frac{2}{5}$
4	$\frac{2}{21}$	$-\frac{2}{21}$
6	$-\frac{2}{45}$	$-\frac{2}{45}$
8	$\frac{2}{77}$	$-\frac{2}{77}$
10	$-\frac{2}{117}$	$-\frac{2}{117}$
12	$\frac{2}{165}$	$-\frac{2}{165}$
14	$-\frac{2}{221}$	$-\frac{2}{221}$
16	$\frac{2}{285}$	$-\frac{2}{285}$
18	$-\frac{2}{357}$	$-\frac{2}{357}$
20	$\frac{2}{437}$	$-\frac{2}{437}$

results were surprising. The maximum errors agree exactly in magnitude as seen in table (2).

Table 2: The first few maximum error terms from the expansion as a function of the order n. The $(\epsilon_n)_c$ values correspond to the cone, $(\epsilon_n)_s$ to the sphere.

n	$(\epsilon_n)_c$	$(\epsilon_n)_s$
0	$\frac{2}{3}$	$-\frac{2}{3}$
2	$\frac{4}{15}$	$-\frac{4}{15}$
4	$\frac{6}{35}$	$-\frac{6}{35}$
6	$\frac{8}{63}$	$-\frac{8}{63}$
8	$\frac{10}{99}$	$-\frac{10}{99}$
10	$\frac{12}{143}$	$-\frac{12}{143}$
12	$\frac{14}{195}$	$-\frac{14}{195}$
14	$\frac{16}{255}$	$-\frac{16}{255}$
16	$\frac{18}{323}$	$-\frac{18}{323}$
18	$\frac{20}{399}$	$-\frac{20}{399}$
20	$\frac{22}{483}$	$-\frac{22}{483}$

The maximum errors over the domain have the form

$$(\epsilon_n)_c = \frac{n+2}{(n+2)^2 - 1} \tag{20}$$

for $n = 0, 2, 4, \ldots$. The relationship between the errors for the cone and the sphere are

$$(\epsilon_n)_c = -(\epsilon_n)_s . \tag{21}$$

A plot of the residual error for 20th order expansions is shown in figure (5). The maximum error for the cone is at the apex (the origin) and the maximum for the sphere is a the equator (the boundary)

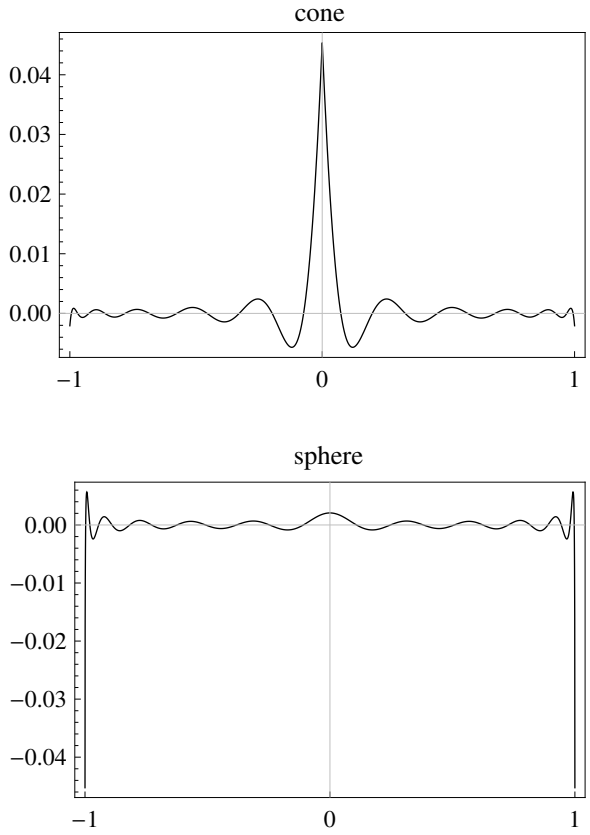

Fig. 5: The residual error for the cone (top) and the sphere (bottom). These curves show the difference between the input surface and the approximating polynomial. The maximum error for the cone is at the vertex; for the sphere it is at the boundary.

3.3 Weierstrass revisited

We have constructed a sequence of C^∞ functions which uniformly approximates a C^0 function over the unit disk $\overline{D}_2$. For the cone,

$$\begin{aligned} A(r) &= 1 - r \\ &= \frac{1}{3} - \sum_{k=1}^{\infty} (-1)^{k+1} \frac{2}{(2k+1)(2k+3)} R^0_{2k}(r), \end{aligned} \tag{22}$$

and for the sphere,

$$\begin{aligned} B(r) &= \sqrt{1 - r^2} \\ &= \frac{2}{3} - \sum_{k=1}^{\infty} \frac{2}{(2k+1)(2k+3)} R^0_{2k}(r). \end{aligned} \tag{23}$$

We are able to explicitly calculate the ϵ in equation (8). To have an approximation error no larger than $\epsilon > 0$, we must go to at least order N where N is the even integer greater

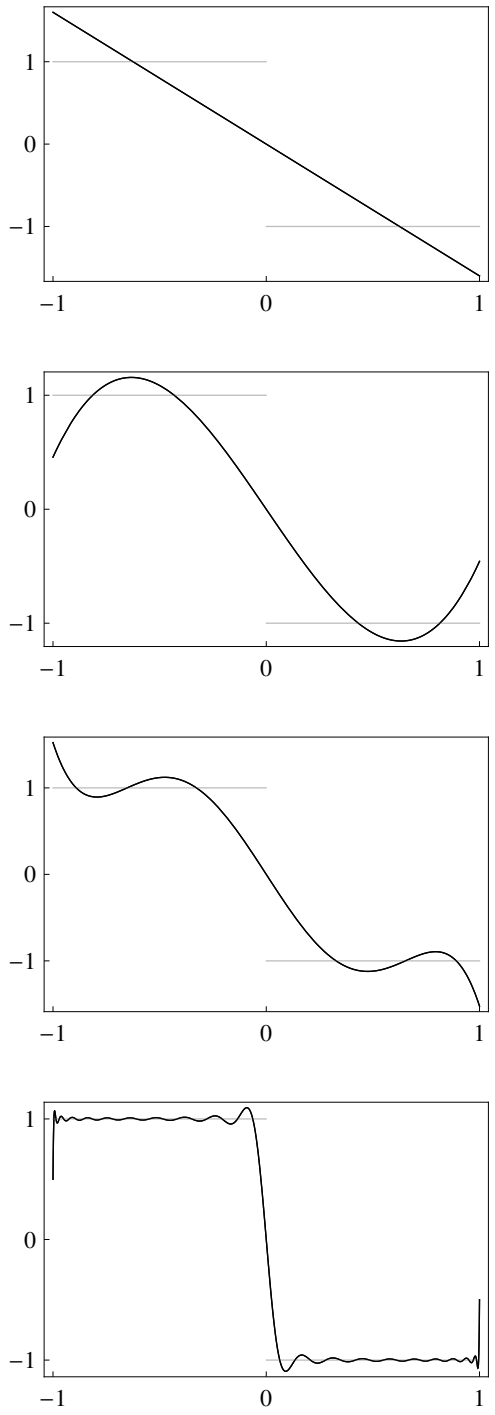

Fig. 6: The first derivative of the approximation (black) for the cone plotted against the first derivative of the input surface (gray). These are the approximations for order $n = 2, 4, 6, 40$. The first derivative is discontinuous at the origin and converges pointwise there.

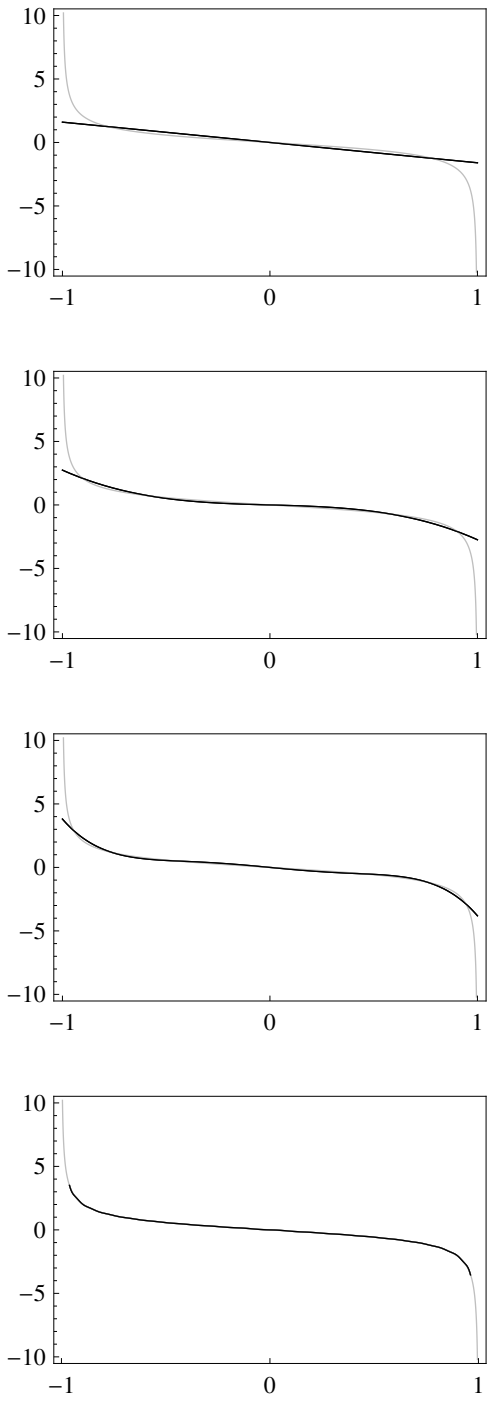

Fig. 7: The first derivative of the approximation (black) for the sphere plotted against the first derivative of the input surface (gray). These are the approximations for order $n = 2, 4, 6, 40$. The first derivative is unbounded at the boundary and converges pointwise there.

than the ceiling of the function shown here:

$$N \geq \left\lceil \frac{1 - 4\epsilon + \sqrt{1 + 4\epsilon^2}}{2\epsilon} \right\rceil. \tag{24}$$

3.4 Pathologies in the first derivative

The location of the maximum error for each surface provides a valuable clue to the seeming paradox presented by the equivalence of the regularity for these very different surfaces. The maximum error for the cone is at the apex where the first derivative is *discontinuous*. For the hemisphere, the maximum error is at the equator where the first derivative is *unbounded*, and therefore discontinuous. We see then that the cone and the sphere both have pathologies in the first derivative.

Let's examine the first derivatives of these figures and the approximation sequence of functions. In figures (6) and (7) we see the first derivatives of the cone and the sphere plotted in gray while the first derivative of the approximation is plotted in black. The first derivative of the cone is a step function with the jump at $r = 0$. While the sphere represents a curve of bounded variation, the first derivative grows without bound as it nears the boundary $|r| = 1$.

4. Conclusion

What have we learned from this study? First, these surfaces have equivalent smoothness in the Zernike basis. In terms of the decay of the expansion amplitudes, the sphere and the cone have exactly the same magnitude at each order. Second, in terms of the maximum error, the sphere and the cone have the exact same magnitude at each order. While we do not explain the exact equivalence shown here, we see that the surfaces are similar because they both have discontinuous first derivatives.

The lesson learned is to be careful about assumptions in approximation theory as the pathologies may be hidden. The pathology of the cone is the discontinuity of the first derivative at the origin and is apparent. The pathology of the sphere is the unbounded growth of the first derivative at the equator and is more subtle.

References

[1] F. Zernike, "Diffraction theory of the knife-edge test and its improved form, the phase-contrast method," *Mon. Not. R. Astron. Soc.*, vol. 94, pp. 377–384, 1934.

[2] M. Born and E. Wolf. *"Principles of Optics : Electromagnetic Theory of Propagation, Interference and Diffraction of Light,"*, 7th ed. Cambridge University Press, 1999.

[3] A. B. Bhatia, and E. Wolf, "On the circle polynomials of Zernike and related orthogonal sets," *Math. Proc. Cam. Phil. Soc.*, vol. 50, pp. 40–48, 1950.

[4] A. Pinkus, "Weierstrass and Approximation Theory," *Journal of Approximation Theory*, vol. 107, pp. 1–66, 2000.